An Asymmetric Carceplex and New Crystal Structure Yield Information Regarding a 1 Million-Fold Template Effect

Janet R. Fraser, Bozena Borecka, James Trotter, and John C. Sherman*

Department of Chemistry, University of British Columbia, Vancouver, British Columbia V6T 1Z1, Canada

Received October 12, 1994[⊗]

We report the incorporation of methyl "feet" as pendant groups in cavitands and carceplexes and their use in the creation of an asymmetric carceplex and the facilitation of the determination of the crystal structure of a carceplex. From the asymmetric carceplex, we have determined a 19 kcal/mol energy barrier to rotation of the guest pyrazine about the host's pseudo-C_2 axes, which demonstrates a high degree of complementarity between the shell of the carceplex and the guest pyrazine. The crystal structure reveals the extensive conjugation of the aryl ethers into the aromatic rings of the host when pyrazine is the guest. This result helps explain why pyrazine is, to date, the best template for the reaction to form the carceplex and thus provides insight to the powerful template effect that is the hallmark of this carceplex reaction. Thus, the investigation of this template effect provides a sensitive probe into noncovalent interactions in general and may be useful in the understanding of recognition in both natural systems such as enzyme/substrate complexes and in non-natural systems such as designed self-assembling structures.

Introduction

Supramolecular assemblies represent a burgeoning field that encompasses myriad areas of science.[1] The assemblies are large, complex systems and require detailed structural characterization for their potential to be fully realized. Carceplexes are supramolecular assemblies that are rigid and well-defined and thus provide ideal platforms from which to study the forces involved in the formation of supramolecular complexes. Carceplexes are closed surface molecules that permanently entrap guest molecules within their shells.[2] The reaction to form carceplex **1a**·guest is subject to an extraordinary template effect where pyrazine is a one million times better template than *N*-methyl-2-pyrrolidinone (NMP).[3] This and 23 other *template ratios* were determined by running the reaction in the presence of two guest/template molecules and measuring the product ratios by integration of the host and guest signals in the ^{1}H NMR spectra of the carceplex mixtures. The template ratios represent the relative rates of the guest-determining step (GDS), the step beyond which no guest exchange occurs. We suggested that one of the driving forces for the reaction is van der Waals interactions of the guest/templates with the walls of the cavity that is formed in the transition state of the GDS.[3] Thus, the investigation of the driving forces to form carceplex **1a**·guest provides a unique opportunity to probe delicate noncovalent interactions as subtle changes in guest size/shape/electronics have a large effect on the template ratios. One crucial element to the elucidation of the template effect in this reaction is the determination of the orientation and mobility of the guests within the shell. This would help expose the relative contributions of the various noncovalent forces (e.g., electrostatic interactions and attractive and repulsive van der Waals interactions) at play in these molecules and may be relevant to the template effect. We report here the determination of the orientation and mobility of the best template molecule, pyrazine, within the carceplex via the study of a new asymmetric carceplex **1c**·pyrazine and the determination

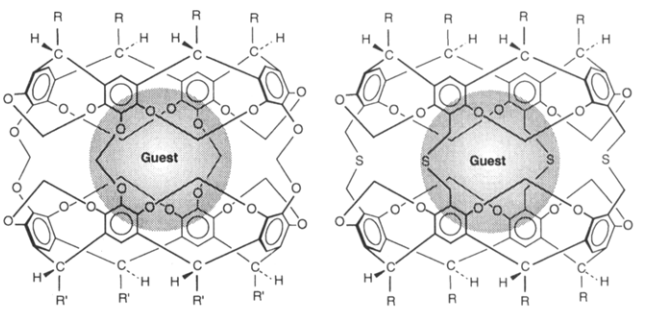

1a: R = R' = CH_2CH_2Ph
1b: R = R' = CH_3
1c: R = CH_3, R' = CH_2CH_2Ph

2a: R = CH_2CH_2Ph
2b: R = CH_3
2c: R = $(CH_2)_4CH_3$

[⊗] Abstract published in *Advance ACS Abstracts,* February 1, 1995.

(1) (a) Lehn, J.-M. *Science* **1993**, *260*, 1762–1763. For self-assembling structures, see: (b) Mathias, J. P.; Simanek, E. E.; Whitesides, G. M. *J. Am. Chem. Soc.* **1994**, *116*, 4326–4340. (c) Bell, T. W.; Jousselin, H. *Nature* **1994**, *367*, 441–444. (d) Zimmerman, S. C.; Murray, T. J. *Tetrahedron Lett.* **1994**, *35*, 4077–4080. (e) Ghadiri, M. R.; Granja, J. R.; Buehler, L. K. *Nature* **1994**, *369*, 301–304. (f) Yang, J.; Marendaz, J.-L.; Geib, S. J.; Hamilton, A. D. *Tetrahedron Lett.* **1994**, *35*, 3665–3668. (g) Drain, C. M.; Fischer, R.; Nolen, E. G.; Lehn, J.-M. *J. Chem. Soc., Chem. Commun.* **1993**, 243–245. (h) Gallant, M.; Viet, M. T. P.; Wuest, J. D. *J. Org. Chem.* **1991**, *56*, 2284–2286. (i) Sessler, J. L.; Magda, D.; Furuta, H. *J. Org. Chem.* **1992**, *57*, 818–826. (j) Carver, F. J.; Hunter, C. A.; Shannon, R. J. *J. Chem. Soc., Chem. Commun.* **1994**, 1277–1280. (k) Wagner, R. W.; Brown, P. A.; Johnson, T. E.; Lindsey, J. L. *J. Chem. Soc., Chem. Commun.* **1991**, 1463–1466. (l) Schall, O. F.; Gokel, G. W. *J. Am. Chem. Soc.* **1994**, *116*, 6089–6100. (m) Menger, F. M.; Littau, C. A. *J. Am. Chem. Soc.* **1993**, *115*, 10083–10090. (n) Watanabe, S.; Regen, S. L. *J. Am. Chem. Soc.* **1994**, *116*, 5762–5765. (o) Müller, A.; Krickemeyer, E.; Dillinger, S.; Bögge, H.; Proust, A.; Plass, W.; Rohlfing, R. *Naturwissenschaften* **1993**, *80*, 560–564. (p) Constable, E. C. *Nature* **1994**, *362*, 412–413. (q) Branda, N.; Wyler, R.; Rebek, J., Jr. *Science* **1994**, *263*, 1267–1268. For assembly via templation, see: (r) Hoss, R.; Vogtle, F. *Angew. Chem., Int. Ed. Engl.* **1994**, *33*, 375–384. (s) Anderson, S.; Anderson, H. L. Sanders, J. K. M. *Acc. Chem. Res.* **1993**, *26*, 469–475. For assembly of imprinted polymers, see: (t) Shea, K. J.; Spivak, D. A.; Sellergren, B. *J. Am. Chem. Soc.* **1993**, *115*, 3368–3369. For assembly of catenanes and rotaxanes, see: (u) Fujita, M.; Ibukuro, F.; Hagihara, H.; Ogura, K. *Nature* **1994**, *367*, 720–723. (v) Amabilino, D. B.; Ashton, P. R.; Reder, A. S.; Spencer, N.; Stoddart, J. F. *Angew. Chem., Int. Ed. Engl.* **1994**, *33*, 433–437. (w) Shen, Y. X.; Xie, D.; Gibson, H. W. *J. Am. Chem. Soc.* **1994**, *116*, 537–548.

(2) Cram, D. J.; Karbach, S.; Kim, Y. H.; Baczynskyj, L.; Marti, K.; Sampson, R. M.; Kalleymeyn, G. W. *J. Am. Chem. Soc.* **1988**, *110*, 2554–2560.

(3) Chapman, R. G.; Chopra, N.; Cochien, E. D.; Sherman, J. C. *J. Am. Chem. Soc.* **1994**, *116*, 369–370.

0022-3263/95/1960-1207$09.00/0 © 1995 American Chemical Society

of the crystal structure of carceplex **1b**·pyrazine. The asymmetric carceplex reveals a remarkably high energy barrier for pyrazine rotation within the shell and reflects the exquisite shape selectivity of the system. For the crystal structure, we describe a new approach that creates more stable crystals of carceplexes and greatly reduces the number of solvate molecules, thus dramatically facilitating the crystal structure determination.

Previously, the only crystal structure of a carceplex was that of **1a**·dimethylacetamide (DMA).[4] The crystal structure of **1a**·DMA was very difficult to solve due to the instability of the crystals and the presence of numerous disordered solvent molecules. To enhance the stability of the crystals and reduce the number of interstitial solvent molecules, we changed the eight large, flexible phenethyl pendant groups to small, fixed methyl groups, although this was counter to the solubility lore that had been established for carceplexes. The first carceplex, **2b**, contained methyl "feet" as the pendant groups and was insoluble in all solvents.[2] The first soluble carceplex, **1a**, contained phenethyl "legs" as the pendant groups and was soluble in chloroform,[4] and since then, all carceplexes[5,6] and hemicarceplexes[7] composed of two resorcinarene units have contained either phenethyl or pentyl "legs". Despite the established insolubility of carceplex **2b**, we report here an investigation of the synthesis, solubility, and crystallinity of carceplex **1b** and compare the solubilities of a series of cavitands and carceplexes with methyl versus phenethyl pendant groups.

Results and Discussion

Solubilities. Carceplex **1a**·pyrazine was prepared as described previously[4] using tetrol **3a**. Carceplex **1b**·pyrazine was prepared by the same method using tetrol **3b**. Carceplex **1c**·pyrazine was prepared using a 1:1

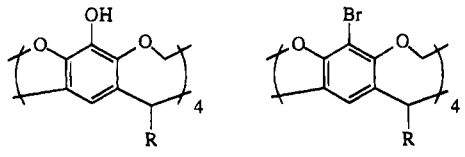

3a: R = CH_2CH_2Ph **4a**: R = CH_2CH_2Ph
3b: R = CH_3 **4b**: R = CH_3

Table 1. Solubility of Cavitands and Carceplexes

compd	solvent	solubility mM	solubility mg/mL
1a	$CHCl_3$	2.8	6.1
1b	$CHCl_3$	13	18
1c	$CHCl_3$	11	20
3a	$CHCl_3$	3.4	3.4
3b	$CHCl_3$	4.4	2.9
4a	$CHCl_3$	92	120
4b	$CHCl_3$	41	38
5a	H_2O	300	330
5b	H_2O	400	300

mixture of tetrols **3a** and **3b** followed by chromatographic separation from carceplexes **1a**·pyrazine and **1b**·pyrazine. The chloroform solubilities of these carceplexes and tetrols and cavitands **4a**[4] and **4b**[8] are shown in Table 1.

The phenethyl cavitand **4a** is two to three times more soluble than the methyl cavitand **4b** in chloroform, depending on whether one compares molarity or weight per volume. The tetrols **3a** and **3b** have comparable solubilities in chloroform. The methyl carceplex **1b**·pyrazine is actually 3–4 times *more* soluble in chloroform than the phenethyl carceplex **1a**·pyrazine and is comparable in solubility to the asymmetric carceplex **1c**·pyrazine. Overall, the solubility of these cavitands and carceplexes in chloroform is largely independent of the apolar pendant group.

We were surprised at these solubilities because carceplex **2b** was reported to be insoluble in any solvent (including chloroform), based on days of Soxhlet extraction with no dissolution,[2] while carceplexes **2a**·guest and **2c**·guest were reported to be soluble in chloroform.[5] Also, we expected, a priori, that four or eight phenethyl groups would dramatically increase the chloroform solubility of such rigid compounds because the phenethyls are large flexible groups that should create less stable packing arrays and should be intrinsically soluble in chloroform (e.g., the values of Hildebrand's δ for chloroform and benzene are 19.0 and 18.8, respectively[9]). One explanation for the insolubility of carceplex **2b** is that the sample was reported to contain a variety of entrapped species including ions, and a large apolar shell containing a buried charge might have unusual solubility. Carceplexes **1a**·guest, **1b**·guest, **1c**·guest, **2a**·guest, and **2c**·guest were never found to contain any ions. We conclude that the prediction of solubilities of these compounds is very difficult and that the widespread use of pentyl or phenethyl legs for the purposes of solubilizing carceplexes[3–6] and hemicarceplexes[7] may be unnecessary.

The water solubility of the cavitand sodium salts **5a** and **5b** was also investigated. These salts were prepared by adding a THF solution of tetrol **3a** or **3b**, respectively, to sodium methoxide in methanol. The solubilities of **5a** and **5b** in water are shown in Table 1, and surprisingly, **5a** and **5b** have similar solubilities. The presence of large apolar groups is apparently inconsequential to water solubility. However, the behavior of these compounds in water is markedly different as the ^1H NMR spectrum of **5b** in D_2O is sharp, well-resolved (Figure 1), and concentration independent. In contrast, the spectrum of **5a**

(4) Sherman, J. C.; Knobler, C. B.; Cram, D. J. *J. Am. Chem. Soc.* **1991**, *113*, 2194–2204.
(5) Bryant, J. A.; Blanda, M. T.; Vincenti, M.; Cram, D. J. *J. Am. Chem. Soc.* **1991**, *113*, 2167–2172.
(6) An asymmetric carceplex composed of a calix[4]arene and a resorcinarene containing $C_{11}H_{23}$ pendant groups has been reported: Timmerman, P.; Verboom, W.; van Veggel, F. C. J. M.; van Hoorn, W. P.; Reinhoudt, D. N. *Angew. Chem., Int. Ed. Engl.* **1994**, *33*, 1292–1295.
(7) (a) Cram, D. J.; Tanner, M. E.; Knobler, C. B. *J. Am. Chem. Soc.* **1991**, *113*, 7717–7727. (b) Robbins, T. A.; Knobler, C. B.; Bellew, D. R.; Cram, D. J. *J. Am. Chem. Soc.* **1994**, *116*, 111–122. (c) Cram, D. J.; Jaeger, R.; Deshayes, K. *J. Am. Chem. Soc.* **1993**, *115*, 10111–10116. (d) Robbins, T. A.; Cram, D. J. *J. Am. Chem. Soc.* **1993**, *115*, 12199. (e) Cram, D. J.; Blanda, M. T.; Paek, K.; Knobler, C. B. *J. Am. Chem. Soc.* **1992**, *114*, 7765–7773. (f) Choi, H.-J.; Bühring, D.; Quan, M. L. C.; Knobler, C. B.; Cram, D. J. *J. Chem. Soc., Chem. Commun.* **1992**, 1733–1735. (g) Timmerman, P.; van Mook, M. G. A.; Verboom, W.; van Hummel, G. J.; Harkema, S.; Reinhoudt, D. N. *Tetrahedron Lett.* **1992**, *33*, 3377–3380. (h) Quan, M. L. C.; Cram, D. J. *J. Am. Chem. Soc.* **1991**, *113*, 2754–2755. (i) Judice, J. K.; Cram, D. J. *J. Am. Chem. Soc.* **1991**, *113*, 2790–2791. (j) Quan, M. L. C.; Knobler, C. B.; Cram, D. J. *J. Chem. Soc., Chem. Commun.* **1991**, 660–662. (k) Cram, D. J.; Tanner, M. E.; Thomas, R. *Angew. Chem., Int. Ed. Engl.* **1991**, *30*, 1024–1027. A hemicarceplex composed of two calix[4]arenes has been reported: Blanda, M. T.; Griswold, K. E. *J. Org. Chem.* **1994**, *59*, 4313–4315.
(8) Cram, D. J.; Karbach, S.; Kim, H.; Knobler, C. B.; Maverick, E. F.; Ericson, J. L.; Helgeson, R. C. *J. Am Chem. Soc.* **1988**, *110*, 2229–2237.
(9) Reichardt, C. *Solvents and Solvent Effects in Organic Chemistry*, 2nd ed.; VCH: New York, 1988; p 58.

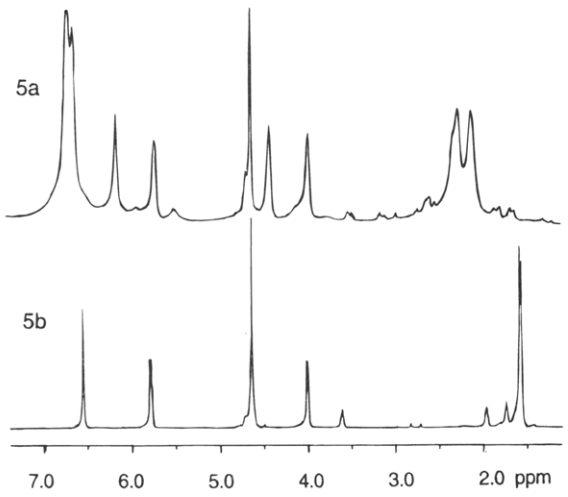

Figure 1. ^{1}H NMR spectra of cavitand salts **5a** and **5b** at 400 MHz in D_2O at 25 °C, 45 mM.

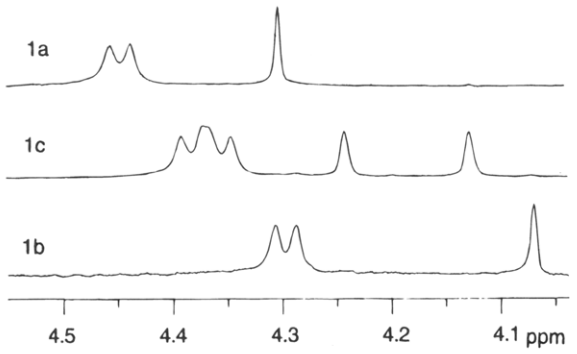

Figure 2. ^{1}H NMR spectra of pyrazine entrapped in carceplex **1a** (4.30 ppm), **1c** (4.24 and 4.13 ppm), and **1b** (4.07 ppm) at 500 MHz in nitrobenzene-d_5 at 25 °C. Host proton signals appear at 4.45, 4.36, and 4.30 ppm for **1a**, **1c**, and **1b**, respectively.

is broad (Figure 1) over a broad range of concentrations,[10] suggesting that the pendant phenethyl groups promote aggregation in water.

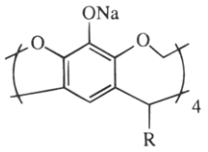

5a: R = CH_2CH_2Ph
5b: R = CH_3

Asymmetric Carceplex 1c·Pyrazine. The anisotropic environment of the cavity of carceplex **1a**·pyrazine is substantially different from that of **1b**·pyrazine as demonstrated by their ^{1}H NMR spectra (Figure 2).[6] The chemical shifts of the guest's protons differ by 0.23 ppm in nitrobenzene-d_5. Moreover, for the asymmetric carceplex **1c**·pyrazine, two guest signals are observed that are separated by 0.11 ppm. Resolution enhancement showed that each signal is a doublet with 1.2 Hz coupling. The different magnetic environments created by the methyl and phenethyl hemispheres in **1c**·pyrazine allows us to make some conclusions about the orientation and

(10) The ^{1}H NMR spectra of **5a** in D_2O are broad from 2.8 to 33 mM, so the critical micelle concentration is likely to be well below 2.8 mM.

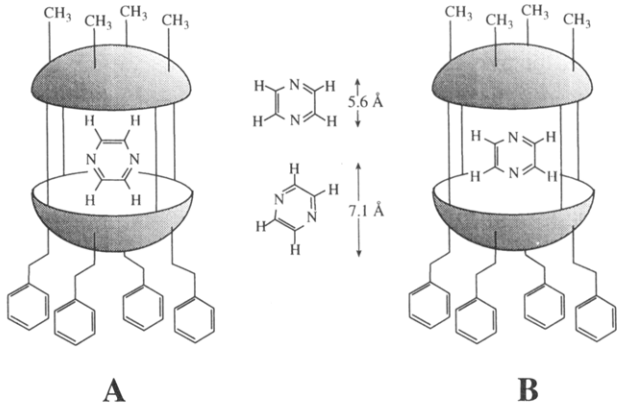

Figure 3. Schematic representation of pyrazine orientation in the cavity of carceplex **1c**. Structure **A** is consistent with the experimental results.

mobility of pyrazine within the shell. For two signals to appear, the pyrazine must sit as shown in Figure 3A with the nitrogens at the equator of the shell and two adjacent protons in each of the methyl and phenethyl hemispheres. An alternative alignment with the nitrogens at the poles of the shell (Figure 3B) would yield two doublets split by a 6−7 Hz *ortho*-coupling due to the anisotropy of the cavity.[11] In fact, **1c**·pyrazine reveals a *meta*-coupling constant[11] of 1.2 Hz that is not normally observed due to the D_{2h} symmetry of pyrazine. This orientation with the pyrazine nitrogens at the equator of the host reflects the complementarity of the host and guest, as the carceplex cavity is significantly narrower at the equator than between the poles while pyrazine is narrower across the 1,4-nitrogens than across the 1,4-carbons (5.6 versus 7.1 Å including van der Waals distances).

Since we observe two well-resolved signals for the guest protons in the ^{1}H NMR spectrum of **1c**·pyrazine, rather than one average signal, we conclude that the pyrazine molecule does not rotate about the pseudo-C_2 axes of the shell on the ^{1}H NMR time scale at 25 °C. At higher temperatures, rotation of pyrazine can occur as shown by the variable temperature 500 MHz ^{1}H NMR spectra of **1c**·pyrazine in nitrobenzene-d_5 (Figure 4). The two pyrazine signals coalesce at 115°C, which corresponds to a 19 kcal/mol energy barrier to pyrazine rotation about the pseudo-C_2 axes of the shell.[12] This energy represents the strain that is imparted to the shell when the equator is forced to accommodate the larger diameter of the guest (7.1 Å versus 5.6 Å) and demonstrates most dramatically the extraordinary size and shape complementarity between pyrazine and the cavity of the carceplex.

Crystal Structure of Carceplex 1b·Pyrazine. The only published crystal structure of a carceplex is that of **1a**·DMA.[4] The crystals were grown from a chloroform/acetonitrile solution and were unstable upon exposure to air such that the crystals instantaneously lost their solvates and turned to powder. X-ray diffraction had to be performed on crystals submerged in their mother liquor and sealed in a capillary tube, since they were not

(11) Silverstein, R. M.; Bassler, G. C.; Morrill, T. C. *Spectrometric Identification of Organic Compounds*, 4th ed.; Wiley: New York, 1981; p 235.

(12) The energy barrier was determined from the coalescence temperature (T_c = 388 K) and the resonance frequency difference in the two protons ($\delta\nu$ = 55 Hz) using the following equation: $\Delta G^{\ddagger} = [22.96 + \ln (T_c/\delta\nu)](RT_c)$. See: Abraham R. J.; Fisher, J.; Loftus, P. *Introduction to NMR Spectroscopy*; Wiley: New York, 1990; pp 194−7.

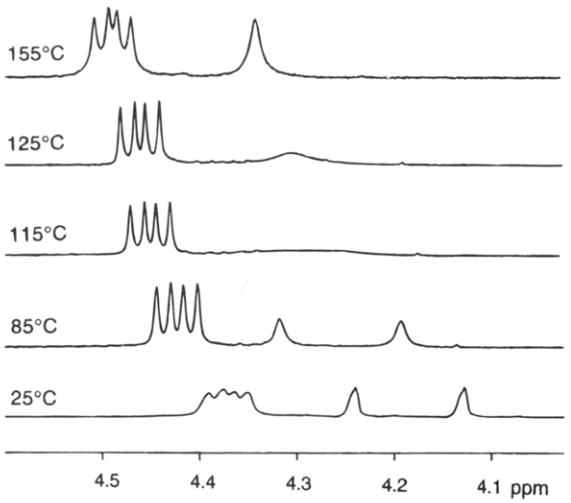

Figure 4. ^{1}H NMR spectra of pyrazine entrapped in carceplex **1c** (4.13 and 4.24 ppm at 25 °C → 4.33 ppm at 155 °C) at 500 MHz in nitrobenzene-d_5 at 25, 85, 115, 125, and 155 °C. The signals ranging from 4.35 to 4.50 ppm are of host protons.

stable enough to be drawn out of solution and coated with silicon rubber. This instability is consistent with the observation of many solvent molecules in the crystal structure, which are required to organize the eight phenethyl legs into a uniform packing array.[4] We expected that the methyl-footed carceplex **1b** would be far more stable, and indeed, crystals of **1b**·pyrazine grown from chloroform/acetonitrile were stable in air indefinitely.[13] Thus, crystals were mounted directly onto a probe after being affixed with silicon rubber and survived 17 days of diffraction. Only two disordered chloroform molecules were present in the asymmetric unit, and the agreement R value is 0.09 compared with 0.18 for **1a**·DMA.[4]

The crystal structure of **1b**·pyrazine (Figure 5) shows that pyrazine sits in the cavity with its nitrogens at the equator of the shell, in agreement with the solution ^{1}H NMR experiments described above. For **1b**·pyrazine, the shell is more symmetric and less distorted than in **1a**·DMA, and we attribute these differences to the change in guest, not the change in pendant groups, although the latter cannot be ruled out. The differences in the shell structures occur in the four $-OCH_2O-$ linkages between the top and bottom bowls. The two bowls are tilted away from each other in **1a**·DMA such that the planes containing the two sets of four interbowl oxygens are 5.2° from parallel.[4] In **1b**·pyrazine, these two planes are within 0.3° of being parallel. In **1a**·DMA, each of the four linkages is conformationally unique which yields an asymmetric, distorted shell.[4] In **1b**·pyrazine, the four interbowl linkages are conformationally equivalent yielding a symmetric shell with a helical twist of 21°.

Template Effects on Carceplex Formation. Pyrazine is a 50 000 times better template than DMA for carceplex formation which means that the GDS is 50 000 times faster with pyrazine than with DMA as the template. This is most likely due to pyrazine's superior van der Waals and other noncovalent interactions with the walls of the cavity formed in the transition state of the GDS, while DMA may impart more strain to the complex formed in the transition state.[3] This notion is consistent with the crystal structure of **1b**·pyrazine which shows that pyrazine allows the interbowl oxygens of the shell to conjugate fully with the aromatic rings, while the crystal structure of **1a**·DMA shows that DMA distorts the shell such that these oxygens are forced somewhat out of conjugation. The conjugation of oxygen with the aromatic ring in anisole is worth 2−3 kcal/mol[14] which suggests that a substantial amount of energy may be gained when pyrazine acts as a template since there are eight aryl ethers involved in the formation of the carceplex. The size/shape/electronic complementarity of pyrazine with the shell of the carceplex is also seen by the large 19 kcal/mol energy barrier to pyrazine rotation about the host's pseudo-C_2 axes.

Other interactions are possible during the templation such as hydrogen bonding between the bowls. We have recently determined the template ratios for the reaction to form hemicarceplex **6**·guest and found that they

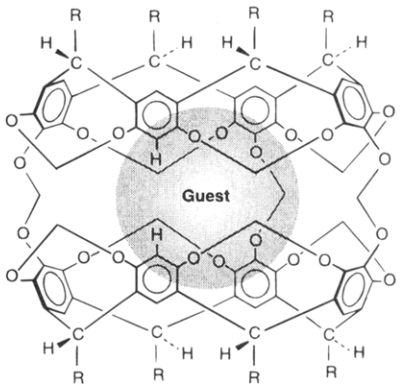

6·Guest: R = CH_2CH_2Ph

correlate nicely with the template ratios for carceplex **1a**·guest.[15] Thus, the driving forces for the two reactions are similar despite the lower symmetry of hemicarceplex **6**·guest. In addition, the yields for carceplex **1a**·guest[3] and for hemicarceplex **6**·guest[7a,15] often exceed the yields expected by statistical analysis. Thus, there is a strong element of self-organization that aligns the bowls for productive bridging.[7a,15] Indeed, we have observed complexes between the template molecules and the bowls of tetrol **3b** where the bowls form hydrogen bonds to each other.[16] We hope that the study of these complexes will help reveal the role of hydrogen bonding and the complementarity of host and guest in the transition state of the GDS.

Conclusions

We have shown the following. (1) Addition of four or eight flexible apolar groups to several rigid apolar compounds does not significantly alter the solubility of these compounds in chloroform. (2) Four large apolar groups do not effect the solubility of a cavitand salt in water, but they do promote aggregation. (3) An asymmetric carceplex reveals the orientation and mobility of the entrapped guest, pyrazine, within the shell. (4) We have developed a general method for creating stable

(13) An interesting note is that although the crystals of **1b**·pyrazine are far more stable (kinetically) than the crystals of **1a**·pyrazine, the two compounds have similar solubilities (a thermodynamic property), which shows that kinetic and thermodynamic properties do not necessarily correlate.

(14) Spellmeyer, D. C.; Grootenhuis, P. D. J.; Miller, M. D.; Kuyper, L. F.; Kollman, P. A. *J. Phys. Chem.* **1990**, *94*, 4483−4491.
(15) Chopra, N.; Sherman, J. C. *Supramol. Chem.*, in press.
(16) Chapman, R. G.; Sherman, J. C. Unpublished results.

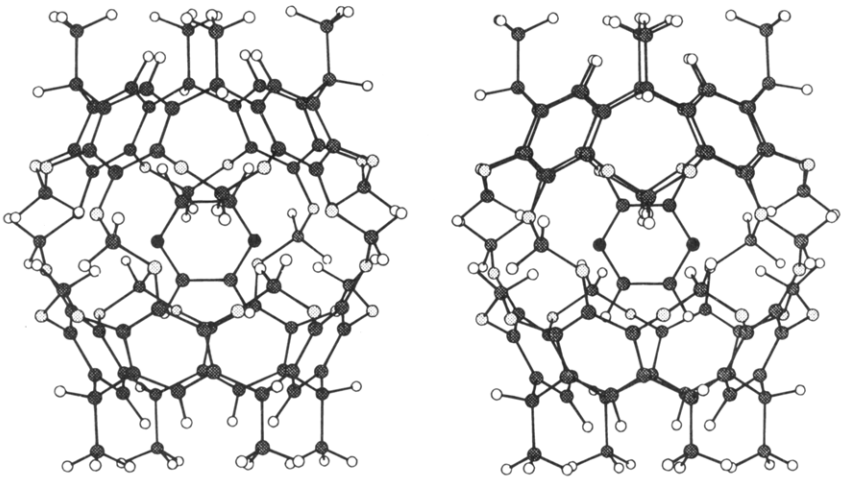

Figure 5. Crystal structure of carceplex **1b**·pyrazine.

crystals of carceplexes and presumably hemicarceplexes, which greatly facilitates the solution of their crystal structures. (5) The pyrazine carceplex is significantly less distorted than the DMA carceplex, which supports the notion that the size/shape/electronic complementarity of pyrazine with the carceplex cavity correlates with pyrazine being a 50 000 times better template than DMA.

Experimental Section

General Procedures. Chemicals were reagent grade (Aldrich or BDH). THF was distilled under N_2 from sodium benzophenone ketyl. *N*-Formylpiperidine was stirred over BaO and then distilled under N_2 onto 4 Å molecular sieves. For ^{1}H NMR spectra, residual ^{1}H signals from deuterated solvents were used as the reference; samples in water were referenced externally to DSS (3-(trimethylsilyl)-1-propanesulfonic acid, sodium salt). Melting points are uncorrected. Silica gel (230−400 mesh, BDH) was used for chromatography, and silica gel glass-backed analytical plates (0.2 mm, Aldrich) were used for TLC; detection was by UV. Dry loading involves dissolution of the solid, addition of silica gel, removal of the solvent in vacuo and loading the solute-adsorbed silica gel onto the column.

1,21,23,25-Tetramethyl-2,20:3,19-dimetheno-1*H*,21*H*,23*H*,25*H*-bis[1,3]dioxocino[5,4-*i*:5′-*i*′]benzo[1,2-*d*:5,4-*d*′]bis[1,3]benzodioxocin-7,11,15,28-tetrol (3b). A suspension of tetrabromide **4b** (1.50 g, 1.7 mmol) in dry THF (500 mL) was warmed until the tetrabromide dissolved. The solution was cooled to −78 °C, and *n*-BuLi (8.8 mL of a 1.5 M solution in hexanes, 13.2 mmol) was added. After 1 min, $B(OMe)_3$ (1.7 mL, 15.0 mmol) was added, and the solution was allowed to warm to ambient temperature over 3 h. The reaction mixture was recooled to −78 °C, 1.5 M NaOH−15% H_2O_2 (45 mL) was added, and the reaction mixture was again allowed to warm to ambient temperature over 3 h. $Na_2S_2O_5$ (10 g, 50 mmol) was carefully added, the THF was removed in vacuo, and the white solid in the residual water was filtered and washed with water. The filtrate was acidified with 10% aqueous HCl and extracted with EtOAc (3 × 60 mL). The combined organic extracts were washed with brine (50 mL), dried with $MgSO_4$, and concentrated in vacuo. The two solids were combined and dry loaded onto a silica gel gravity column that was eluted with EtOAc:hexanes (3:1), affording tetrol **3b**, which was dried at 110°C (0.1 mm Hg) for 24 h (500 mg, 46%): mp >300 °C; ^{1}H NMR (200 MHz, $(CD_3)_2CO$) δ 1.73 (d, 12 H, J = 7.5 Hz), 4.38 (d, 4 H, J = 7.3 Hz), 4.87 (q, 4 H, J = 7.5 Hz), 5.80 (d, 4 H, J = 7.3 Hz), 7.11 (s, 4H), 7.86 (s); MS (LSIMS+, NOBA) m/e 656 (M^+, 100). Anal. Calcd for $C_{36}H_{32}O_{12}$: C, 65.83; H, 4.91. Found: C, 65.50; H, 5.08.

Pyrazine Complex with 1,19,21,29,47,49,57,62-Octamethyl-13,59:41,60-bis(epoxymethanoxy)-23,27:51,55-dimethano-2,46:3,45:17,31:18,30-tetrametheno-1*H*,19*H*,21*H*,29*H*,47*H*,49*H*-bis[1,3]benzodioxocino[9,8-*d*:9′-*d*′][1,3,6,8,11,13,16,18]octaoxacycloeicosino[4,5-*j*:10,9-*j*′:14,15-*j*′:20,19-*j*′]tetrakis[1,3]benzodioxocin (1:1) (1b·Pyrazine). A mixture of tetrol **3b** (100 mg, 0.15 mmol), pyrazine (60 mg, 0.75 mmol), K_2CO_3 (414 mg, 3.0 mmol), and CH_2BrCl (100 μL, 1.5 mmol) in *N*-formylpiperidine (40 mL) was maintained at 60 °C for 24 h. An additional 100 μL of CH_2BrCl was added, and heating was continued for 24 h. The reaction mixture was concentrated in vacuo, water (50 mL) was added, and the resulting slurry was acidified with 10% aqueous HCl. The slurry was extracted with $CHCl_3$ (3 × 60 mL), and the combined organic fractions were washed with brine (50 mL), dried with $MgSO_4$, and concentrated in vacuo. The residue was dry loaded onto a silica gel gravity column that was eluted with $CHCl_3$:hexanes (3:1), affording **1b·pyrazine**, which was dried at 110 °C (0.1 mm Hg) for 24 h (96 mg, 87%): mp >300 °C; ^{1}H NMR (200 MHz, $CDCl_3$) δ 1.76 (d, 24 H, J = 7.4 Hz), 3.99 (s, 4 H), 4.24 (d, 8 H, J = 7.6 Hz), 5.01 (q, 8 H, J = 7.4 Hz), 6.01 (d, 8 H, J = 7.6 Hz), 6.44 (s, 8 H), 7.00 (s, 8H); MS (DCI, isobutane) m/e 1442 ($M + H^+$, 100). Anal. Calcd for $C_{80}H_{68}N_2O_{24}$: C, 66.66; H, 4.76; N, 1.94. Found: C, 66.50; H, 4.74; N, 1.80.

Pyrazine Complex with 1,47,49,57-Tetramethyl-19,21,29,62-tetrakis(2-phenylethyl)-13,59:41,60-bis(epoxymethanoxy)-23,27:51,55-dimethano-2,46:3,45:17,31:18,30-tetrametheno-1*H*,19*H*,21*H*,29*H*,47*H*,49*H*-bis[1,3]benzodioxocino[9,8-*d*:9′-*d*′][1,3,6,8,11,13,16,18]octaoxacycloeicosino[4,5-*j*:10,9-*j*′:14,15-*j*′:20,19-*j*′]tetrakis[1,3]benzodioxocin (1:1) (1c·Pyrazine). A mixture of tetrol **3a** (93 mg, 0.090 mmol), tetrol **3b** (60 mg, 0.090 mmol), pyrazine (90 mg, 1.12 mmol), K_2CO_3 (490 mg, 3.6 mmol), and CH_2BrCl (150 μL, 2.25 mmol) in *N*-formylpiperidine (80 mL) was maintained at 60 °C for 24 h. An additional 50 μL of CH_2BrCl was added, and heating was continued for 24 h. The reaction mixture was concentrated in vacuo, water (50 mL) was added, and the resulting slurry was acidified with 10% aqueous HCl. The slurry was extracted with $CHCl_3$ (3 × 60 mL), and the combined organic fractions were washed with brine (50 mL), dried ($MgSO_4$), and concentrated in vacuo. The residue was dry loaded onto a silica gel gravity column that was eluted with $CHCl_3$:hexanes (7:3), affording **1a·pyrazine** (11 mg, 7%), **1b·pyrazine** (10 mg, 10%), and **1c·pyrazine** (23 mg, 9%), which were dried at 110 °C (0.1 mm Hg) for 24 h. **1c·pyrazine** was characterized: mp >300 °C; ^{1}H NMR (400 MHz, $CDCl_3$) δ 1.76 (d, 12 H, J = 7.4 Hz), 2.49−2.53, 2.64−2.68 (m, 16 H), 4.01 (d, 2 H, J = 1.2 Hz), 4.05 (d, 2 H, J = 1.2 Hz), 4.25 (m, 8 H), 4.89 (t, 4 H, J = 7.8 Hz), 5.02 (q, 4 H, J = 7.4 Hz), 6.02 (m, 8 H), 6.45 (s, 8 H), 6.91 (s, 4H), 7.00 (s, 4H), 7.13−7.22 (m, 20 H); MS (DCI, isobutane) m/e 1803 ($M + H^+$, 100). Anal. Calcd for $C_{108}H_{92}N_2O_{24}$: C, 71.99; H, 5.15; N, 1.55. Found: C, 71.86; H, 5.06; N, 1.50.

Tetrasodium Salt of 1,21,23,25-Tetramethyl-2,20:3,19-dimetheno-1*H*,21*H*,23*H*,25*H*-bis[1,3]dioxocino[5,4-*i*:5′-*i*′]-

Table 2. Crystal Data and Structure Refinement for 1b·Pyrazine

A. Crystal Data	
formula	$C_{76}H_{64}O_{24}{\cdot}C_4H_4N_2{\cdot}1^1/_3(CHCl_3)$
formula w	1600.6
cryst color, habit	colorless, prism
cryst size	0.2 × 0.2 × 0.2 mm
no. of reflns used for unit cell determination (2θ range)	25 (38.4–54.4°)
ω scan peak width at half-ht	0.39
cryst system	monoclinic
space grp	$P2_1/n$
unit cell dimens	a = 14.243(2) Å, α = 90°
	b = 21.679(4) Å, β = 94.842(8)°
	c = 33.658(2) Å, γ = 90°
volume	10 356(2) Å^3
Z	6
density (calcd)	1.540 mg/m^3
absorption coeff	23.2 cm^{-1}
F(000)	4988
B. Intensity Measurements	
diffractometer	Rigaku AFC6S
radiatn Cu Kα (λ = 1.541 78 Å)	graphite monochromatized
take-off angle	6.0°
detector aperture	6.0 mm horizontal
	6.0 mm vertical
cryst to detector dist	285 mm
temp	294 K
scan type	$\omega - 2\theta$
scan rate	16.0°/min (in ω) (up to nine scans)
scan width	(0.95 + 0.20 tan θ)°
$2\theta_{max}$	155.2°
index ranges	h = 0–17, k = 0–27, l = −42 to 42
no. of reflns measured	total: 22954
	unique: 21449 (R_{int} = 0.059)
corrections	Lorentz polarization
	absorption (trans. factors: 0.80–1.0)
	decay (1.98%)
C. Structure Solution and Refinement	
struct soln	direct methods (SHELXS86)
refinement method	block least-squares on F^2 (SHELXL93)
data/restraints/parameters	21441/66/2097 (five blocks)
weighting scheme	$1/[\sigma^2(F_o^2) + (0.1564P)^2 + 6.852P]$ where $P = [\max(F_o^2,0) + 2F_c^2]/3$
goodness-of-fit on F^2	1.047
final R indices [$I > 2\sigma(I)$, 8258 reflns]	R_1 = 0.0937, wR_1 = 0.2649
R indices (all data)	R_2 = 0.2514, wR_2 =0.3383
extinction coeff	0.001 07(8)
largest diff peak and hole	0.51 and −0.68 e·Å^{-3}
max D/esd	0.31
mean D/esd	0.05

benzo[1,2-*d*:5,4-*d*′]bis[1,3]benzodioxocin-7,11,15,28-tetrol (5b). A solution of tetrol **3b** (79 mg, 0.12 mmol) in THF (50 mL) was added to 1.0 M sodium methoxide in methanol (0.6 mL, 0.60 mmol), and the reaction mixture was stirred for 2 h. The reaction mixture was concentrated in vacuo, and THF (30 mL) was added. This procedure was repeated three times before the suspension was filtered through a fine frit. The tan solid was washed with THF (10 mL) and dried at 78 °C (0.1 mm Hg) for 4 d, affording tetrasodium salt **5b** (75 mg, 83%). Tetrol **3b** could be regenerated by acidification of an aqueous solution of tetrasodium salt **5b** with 5% HCl and extraction with EtOAc. Tetrasodium salt **5b** was characterized: ^{1}H NMR (400 MHz, D_2O, 45 mM) δ 1.57 (d, 12 H, J = 7.2 Hz), 4.00 (d, 4 H, J = 7.1 Hz), 4.63 (br), 5.77 (d, 4 H, J = 7.1 Hz), 6.54 (s, 4 H).

Tetrasodium Salt of 1,21,23,25-Tetrakis(2-phenylethyl)-2,20:3,19-dimetheno-1*H*,21*H*,23*H*,25*H*-bis[1,3]dioxocino[5,4-*i*:5′-*i*′]benzo[1,2-*d*:5,4-*d*′]bis[1,3]benzodioxocin-7,11,15,28-tetrol (5a). A solution of tetrol **3a** (100 mg, 0.10 mmol) in THF (60 mL) was subjected to the preceding procedure, affording tetrasodium salt **5a** (94 mg, 86%). Tetrol **3a** could be regenerated by acidification of an aqueous solution of tetrasodium salt **5a** with 5% HCl and extraction with EtOAc. Tetrasodium salt **5a** was characterized: ^{1}H NMR (400 MHz, D_2O, 45 mM) δ 2.11–2.33 (m, 16 H), 3.97 (br s, 4 H), 4.42 (br s), 5.71 (br s, 4 H), 6.16 (br s, 4 H), 6.64–6.71 (m, 20 H).

Typical Chloroform Solubility Measurement. Cavitand **4b** (95 mg, 0.11 mmol) was dissolved in refluxing $CHCl_3$ (2.5 mL), yielding a clear solution, and this was allowed to slowly cool to room temperature. The precipitate formed was removed by filtration through a 45 μm nylon filter, and a 1.20 mL sample of the saturated filtrate was allowed to stand at room temperature for 1 h. The $CHCl_3$ was evaporated under a stream of N_2, and the residue was dried at 110 °C (0.1 mmHg) for 24 h. The dried residue weighed 45.1 mg, giving a solubility of 37.6 mg/mL, 41 mM. Errors are estimated to be ±20%.

Typical Water Solubility Measurement. Cavitand salt **5a** (35 mg, 0.032 mmol) was added to 80 μL of distilled water, and the mixture was sonicated in a room temperature water bath for 20 min. The solution was passed through a 45 μm nylon filter, and a 30 μL sample was removed. The water was evaporated under a stream of N_2, and the residue was dried at 78 °C (0.1 mmHg) for 24 h. The dried residue weighed 9.8 mg, giving a solubility of 330 mg/mL, 300 mM.

Crystal Structure of 1b·Pyrazine. **1b**·pyrazine crystallizes from chloroform/acetonitrile as colorless prisms and forms unusually stable crystals. Full experimental details are given in Table 2.

The structure was solved by direct methods,[17] expanded using Fourier Difference techniques, and refined by least-squares methods. The unit cell contains six carceplex and six

(17) SHELXS-86: Sheldrick, G. M. In *Crystallographic Computing 3*; Sheldrick, G. M., Kruger, C., Goddard, R., Eds.; Oxford University Press: Oxford, 1985; pp 175–189.

pyrazine guest molecules (four of each in general positions and two of each disordered on centers of symmetry) and eight chloroform solvate molecules; the asymmetric unit is one ordered carceplex and pyrazine guest disordered over two sites, a half of carceplex and pyrazine (both disordered over two sites), and two $CHCl_3$ (both disordered over two sites).

The host molecule contains the pyrazine molecule in the cavity created by four bridging OCH_2O groups. The pyrazine is disordered over two nearly perpendicular positions with an occupancy of 0.5. Nitrogen atoms are located at the equatorial positions. There are two molecules of chloroform outside the carceplex cavity area. One molecule of chloroform is disordered over two positions refined with an occupancy of 0.7 and 0.3, respectively. The other has two disordered positions with an occupancy of 0.5. It is possible that the disorder models for the chloroform solvent are not sufficient to describe the observed electron density in this area, as suggested by the residual peaks in the difference Fourier map and the large atomic displacement parameters for the chlorine atoms.

The final cycle of block least-squares refinement on F^2 was based on 21 441 independent reflections and 2097 variable parameters and converged (largest parameter shift was 0.31 times its esd) to a final agreement factor[18] $R_1 = 0.094$.

All calculations were performed using teXsan[19] and SHELXL93.[20]

Acknowledgment. We thank the University of British Columbia and the Natural Sciences and Engineering Research Council of Canada (NSERC) for financial support. J.R.F. thanks NSERC for a Fellowship via the Bilateral Exchange Program with the Royal Society. Acknowledgment is made to the donors of the Petroleum Research Fund, administered by the American Chemical Society, for partial support of this research. We thank Professor Jay Siegel for helpful discussions regarding the conjugation in aryl ethers.

JO941708X

(18) Least-squares refinement on F^2 for all reflections except for eight with very negative F2 or flagged by the user for potential systematic errors. Weighted R factors wR_2 and all goodnesses of fit S are based on F^2, conventional R factors R_1 are based on F, with F set to zero for negative F^2. The observed criterion of $F^2 > 2\sigma(F^2)$ is used only for calculating R factors and is not relevant to the choice of reflections for refinement. The author has deposited atomic coordinates for **1b**·pyrazine with the Cambridge Crystallographic Data Centre. The coordinates can be obtained, on request, from the Director, Cambridge Crystallographic Data Centre, 12 Union Road, Cambridge, CB2 1EZ, UK.

(19) teXsan: Crystal Structure Analysis Package, Molecular Structure Corp., 1985 and 1992.

(20) SHELXL-93: Sheldrick, G. M. *J. Appl. Crystallogr.* **1993**, manuscript in preparation.